Membrane-Induced Folding and Structure of Membrane-Bound Annexin A1 N-Terminal Peptides: Implications for Annexin-Induced Membrane Aggregation

Nien-Jen Hu,*† Jeremy Bradshaw,‡ Hans Lauter,§ Julia Buckingham,¶ Egle Solito,¶ and Andreas Hofmann*‖

*Institute of Structural and Molecular Biology, School of Biological Sciences, The University of Edinburgh, Edinburgh EH9 3JR, United Kingdom; †Division of Molecular Biosciences, Department of Biological Sciences, Imperial College, London SW7 1LU, United Kingdom; ‡Royal (Dick) School of Veterinary Studies, The University of Edinburgh, Easter Bush Veterinary Centre, Roslin, Midlothian EH25 9RG, United Kingdom; §Institut Laue-Langevin, BP 156, 38042 Grenoble Cedex 9, France; ¶Neuroendocrine Unit, Department of Cellular and Molecular Neuroscience, Hammersmith Hospital, Imperial College, London W12 0NN, United Kingdom; and ‖Structural Chemistry Program, Eskitis Institute for Cell and Molecular Therapies, Griffith University, Brisbane 4111, Australia

ABSTRACT Annexins constitute a family of calcium-dependent membrane-binding proteins and can be classified into two groups, depending on the length of the N-terminal domain unique for each individual annexin. The N-terminal domain of annexin A1 can adopt an α-helical conformation and has been implicated in mediating the membrane aggregation behavior of this protein. Although the calcium-independent interaction of the annexin A1 N-terminal domain has been known for some time, there was no structural information about the membrane interaction of this secondary membrane-binding site of annexin A1. This study used circular dichroism spectroscopy to show that a rat annexin A1 N-terminal peptide possesses random coil structure in aqueous buffer but an α-helical structure in the presence of small unilamellar vesicles. The binding of peptides to membranes was confirmed by surface pressure (Langmuir film balance) measurements using phosphatidylcholine/phosphatidylserine monolayers, which show a significant increase after injection of rat annexin A1 N-terminal peptides. Lamellar neutron diffraction with human and rat annexin A1 N-terminal peptides reveals an intercalation of the helical peptides with the phospholipid bilayer, with the helix axis lying parallel to the surface of membrane. Our findings confirm that phospholipid membranes assist the folding of the N-terminal peptides into α-helical structures and that this conformation enables favorable direct interactions with the membrane. The results are consistent with the hypothesis that the N-terminal domain of annexin A1 can serve as a secondary membrane binding site in the process of membrane aggregation by providing a peripheral membrane anchor.

INTRODUCTION

Since the 1980s, annexins have been discovered in different taxonomic kingdoms, with the best-studied subfamily being the one from vertebrate animals, now designated annexin group A. Members of this protein family are involved in membrane trafficking and reorganization as well as in processes such as endo-, exo-, and phagocytosis (1,2).

Annexins are ubiquitous in cytosolic proteins, and their members share the property of calcium-dependent binding to membranes containing negatively charged phospholipids (3–6), which underpins their biological functions on the cytoplasmic leaflet of membranes where acidic phospholipids are enriched. Annexins are furthermore involved in the calcium-dependent organization of the cytoskeleton (7) and membrane microdomains (rafts) (8). In the sarcolemma of smooth muscle cells, annexin A2 can promote clustering of phospholipids, stabilize lipid rafts, and thus regulate transmembrane signal transduction (9).

Calcium ions are coordinated in type II (10,11) or type III (12) binding sites. The bound calcium ions in type II and type III binding sites serve as a bridge to enable annexin interactions with phospholipid membranes (13,14). The circular array of four repeats yields the shape of a curved disk for the C-terminal domain. The N-terminal domain is located on the concave side of annexins and varies in length and sequence. It is thus believed to confer specific properties on an individual annexin. A comparison of the length of the N-terminal regions reveals three main groups: between 11 and 19 residues (annexins A3, A4, A5, A6, A10, A12, A13), between 33 and 42 residues (annexins A2 and A1, respectively), and more than 100 residues (annexins A7 and A11). Annexins with considerably longer N-terminal domains have been shown to harbor different phosphorylation sites for serine/threonine and tyrosine-specific kinases as well as binding sites for S100 proteins, e.g., annexin A1, S100A11 (15,16); annexin A2, S100A10 (17); and annexin A11, S100A6 (18).

Annexin A1 is of pharmaceutical interest because it is upregulated by antiinflammatory glucocorticoids and functions as a cellular mediator of glucocorticoids (19). Previous studies have shown that annexin A1 can interact with the phospholipid monolayer in the absence of calcium under acidic conditions (20). Whereas annexin A1, but not annexin A5, was found to aggregate neutrophil and chromaffin cell granules (21,22) as well as phospholipid vesicles (23), a chimera protein with the annexin A1 N-terminal domain fused to the annexin A5 C-terminal domain restored the

Submitted August 13, 2007, and accepted for publication October 22, 2007.

Address reprint requests to Andreas Hofmann, Structural Chemistry Program, Eskitis Institute for Cell and Molecular Therapies, Griffith University, N75 Don Young Road, Nathan, Qld 4111, Australia. Tel.: 61-7-3735-6086; Fax: 61-7-3735-6001; E-mail: a.hofmann@griffith.edu.au.

Editor: Paul H. Axelsen.

0006-3495/08/03/1773/09 $2.00

doi: 10.1529/biophysj.107.119685

aggregation behavior (24). It has thus been concluded that the N-terminal domain of annexin A1 can interact with membranes independently of the canonical annexin membrane binding at the convex surface (25,26). This hypothesis is further supported by the finding that endosome association of annexin A1 requires an intact N-terminal domain (27) as well as the results from a vesicle aggregation study using various annexin A1 truncation mutants (28).

Despite the established involvement of the N-terminal domain, the molecular mechanisms of annexin A1-induced membrane aggregation remain unclear. Two models have been suggested. The first model assumes membrane aggregation is conducted simultaneously by two membrane binding sites on one annexin molecule (21,24,29,30). The second model suggests that an annexin-annexin complex linked via the N-terminal tails or other binding partners, such as S100 proteins, promotes aggregation of two opposite membranes (16,21,29,31).

The crystal structures of full-length annexin A1 in the absence (32) and presence (33) of calcium suggest a calcium-dependent relocation of the N-terminal tail. In the apo-form (32), the N-terminal 26 amino acids fold into two α-helices with a tilt at Glu-17 and insert into the third repeat of the C-terminal domain. Residues 2–12 adopt an amphipathic conformation. The amphipathic character of the N-terminal helix suggests a direct interaction of the N-terminal domain with membrane, possibly by annealing to the lipid surface. In the crystal structure of the calcium-bound form (33), the N-terminal domain was not found in its previous position, i.e., expelled from the third domain. Although the electron density of residues 1–40 could not be resolved, presumably because of the high flexibility of this region, a previous NMR and CD study (34) reported a helical conformation of human annexin A1(2–26) in membrane-mimetic environments.

In this study, we investigate the folding properties and membrane binding behavior of annexin A1 N-terminal peptides. Using CD spectroscopy, we find that the presence of phospholipid vesicles induces an α-helical fold in the rat N-terminal peptide. Calcium-independent interactions of the peptides with membrane monolayers were confirmed with surface film balance measurements. The membrane-binding mode was characterized at the molecular level using neutron diffraction and revealed a parallel orientation of the peptides lying on the surface of membrane. Therefore, the N-terminal domain may serve as a secondary membrane binding site in the process of membrane aggregation. These data support a model of annexin A1-induced membrane aggregation where the protein interacts with two adjacent membrane surfaces simultaneously.

MATERIALS AND METHODS

Proteins and peptides

The cDNA for annexin A1 was kindly provided by Joannes Sri Widada (see 35). Annexin A1 cloned into pKK233-2 was expressed in *Escherichia coli* JM109. The chimera annexin $A1_N$-$A5_C$ was subcloned from pGEXT2T (36) into pRSET_6c (*Nde*I/*BamH*I). Annexin A5 in pRSET_5d, as well as the chimera, were expressed in *E. coli* BL21(DE3). For all proteins, a total of 8 liters of LB medium (50 mg/ml ampicillin) were inoculated with an overnight culture of 1 liter. The cells were grown at 37°C until the OD at 600 nm reached 1.0. Induction was carried out with 0.5 mM isopropyl thio-β-D-galactoside; at that time, the ampicillin concentration was increased twofold, and the temperature was reduced to 30°C. Protein expression proceeded overnight.

Purification of annexin A1 followed the procedure published by Sri Widada and associates (35) with minor modifications. Annexin A5 and the chimera were purified based on the protocol by Burger (37) with minor modifications (38,39). After harvest, cells were lysed by multiple freeze-thaw cycles and subsequent sonication. The resulting suspension was cleared by ultracentrifugation (100,000 $\times$ g, 30 min, 4°C), and the cytosolic fraction was used for further purification. Annexin A1 was subjected to anion-exchange chromatography with Q-Sepharose; appropriate fractions were pooled and dialyzed against 100 mM NaCl, 2 mM $CaCl_2$, 20 mM TRIS (pH = 8.0). Further purification made use of the calcium-dependent lectin behavior of the protein. The solution was loaded onto heparin Sepharose, and annexin A1 eluted with 4 mM EDTA after extensive washing (2 mM $CaCl_2$).

Annexin A5 and the chimera were purified by calcium-dependent binding to liposomes made from soy lipid extract (Lipid Products, Surrey, UK). Briefly, the cytosolic fraction from the ultracentrifugation step was mixed with the liposome suspension, and the calcium concentration was adjusted to 5 mM. Subsequent wash and desorption steps involved several rounds of ultracentrifugation at 5 mM $CaCl_2$, 10 mM EDTA, and 10 mM EDTA/CHELEX. The semipurified annexins were subjected to final anion exchange chromatography with Q-Sepharose.

The peptides (Fig. 1) containing the human annexin A1 sequence were synthesized by Neosystem Laboratory, Strasburg, France. The peptides containing the rat sequences were synthesized by the Advanced Biotechnology Centre Imperial College, London, UK.

Preparation of vesicles

Multilamellar vesicles (MLVs) were prepared following the method of Szoka and Papahadjopoulos (40). Appropriate amounts of pure lipid or lipid mixtures were dissolved in chloroform/methanol (2:1, v/v) followed by evaporation using a nitrogen gas stream. The dry lipid film was deposited under a vacuum system for 12 h to remove the residual organic solvents. The appropriate aqueous buffer was then added to resuspend the dry lipid film by vigorous vortexing and left to settle for 30 min. Throughout the entire process, the temperature of the mixture was maintained above the transition temperature of the lipids.

Dispersion of MLVs using sonication yields small unilamellar vesicles (SUVs) with diameters ranging from 15 to 50 nm. The SUV preparation procedure was modified from Pagano and Weinstein (41). Appropriate amounts of dimyristoyl-phosphatidylcholine (DMPC) and dimyristoyl-phosphatidylserine (DMPS) in a molar ratio of 3:1 were loaded in a round-bottom test tube and dissolved thoroughly in chloroform/methanol (2:1, v/v).

A sample of MLVs with a final phospholipid concentration of 10 mg/ml was prepared according to the procedure above, and a temperature of 35°C was maintained throughout. Subsequently, bath sonication was performed to disperse the MLVs and convert to SUVs. Sonication was performed at 4°C under nitrogen to avoid oxidative degradation of the phospholipids. SUV formation was considered to be completed when the suspension adopted a clear bluish color.

Circular dichroism spectroscopy

For CD measurements, annexin A1 N-terminal peptides were dissolved in buffer consisting of 10 mM NaH_2PO_4 (pH = 6.2) at a final concentration of 0.08 mg/ml. DMPC/DMPS (3:1 molar ratio) SUVs were added to the peptide solution at a molar ratio of n(phospholipid):n(peptide) = 100:1. All sample spectra were corrected by subtracting buffer/SUV-only spectra of

(a)

```
                1       10        20        30        40        50
                |       |         |         |         |         |
human (1-21)    MAMVSEFLKQAWFIENEEQEY
rat   (2-26)     AMVSEFLKQACYIEKQEQEYVQAVK
rat   (1-50)    MAMVSEFLKQACYIEKQEQEYVQAVKSYKGGPGSAVSPYPSFNPSSDVAA
rat   (1-50)S27A MAMVSEFLKQACYIEKQEQEYVQAVKAYKGGPGSAVSPYPSFNPSSDVAA
rat   (1-50)S45A MAMVSEFLKQACYIEKQEQEYVQAVKSYKGGPGSAVSPYPSFNPASDVAA
```

(b)

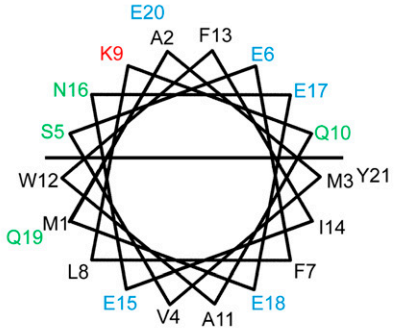

(c)

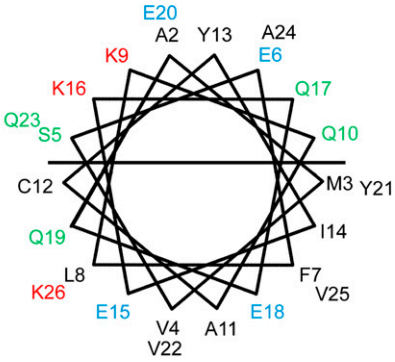

FIGURE 1 (*a*) Peptides used within this study. Helical wheel representation of the N-terminal domains of (*b*) human and (*c*) rat annexin A1 showing the amphipathic character of the α-helix. The horizontal lines indicate the separation of hydrophobic (*down*) and hydrophilic (*up*) faces. The diagrams are produced with WinPep v3.01 (65).

samples containing no peptide. Baseline subtraction and secondary structure prediction were carried out using the program ACDP (42,43).

Monolayer surface pressure measurements

Kinetic studies of peptide adsorption to phospholipid monolayers were carried out on a computer-controlled Langmuir film balance (NIMA) at 20°C. The area of the Teflon trough was 300 cm^2 (30 cm $\times$ 10 cm), and it was equipped with a movable barrier that allowed the adjustment of the surface area of the monolayer. The subphase buffer containing 100 mM NaCl and 20 mM MES (pH = 6.0) was filtered with Whatman 0.1- μm filter paper and poured into the trough until the surface was 2 mm higher than the trough brim (210 ml). The surface of the buffer was separated by the movable barrier into two isolated areas. For optimal circulation and mixture, an extra stirrer made of Teflon, rotating at 6 rpm, was applied in the compartment where no phospholipids were added. The surface pressure was measured with a surface potential meter using 1 cm $\times$ 2.3 cm plates cut from filter paper (Whatman, No. 1). The lipid suspension was prepared as a mixture of DMPC and DMPS (3:1 molar ratio) dissolved in chloroform/methanol (2:1, v/v) at a concentration of 1 mg/ml, and 30 μl of this suspension was applied onto the surface of the subphase with a Hamilton syringe. After spreading, the monolayer was left to equilibrate for 20 min. The film was compressed by moving the barrier to generate a surface pressure of 10 mN/m, a value that is thought to mimic the biological membrane condition (20,44). After 5 min of further equilibration, peptides or proteins were injected into the subphase to a final concentration of 30 nM, using a Hamilton syringe extending beneath the barrier. The surface pressure (mN/m) against time (s) was recorded until no further increase was observed.

Neutron diffraction

Sample preparation and data collection

Multiple bilayers of phospholipids and peptides were prepared following a published protocol (45,46): 20 mg of a DMPC/DMPS mixture (3:1 molar ratio) were codissolved with 1 mol % peptide in chloroform:methanol (2:1, v/v). The solution was airbrushed onto quartz microscope slides using nitrogen as the propellant. The slides were placed under vacuum for 12 h to remove the organic solvent and the samples rehydrated in sealed sample cans for 12 h at 30°C to achieve full equilibration. The relative humidity inside the sample cans was adjusted to 85%, 90%, or 95% by changing the temperature of the water bath. The ^2H_2O concentration was set to 8% (v/v) for each relative humidity. An extra condition was prepared with 50% (v/v) ^2H_2O at 90% relative humidity. Diffraction data sets consisting of five orders of diffraction were collected for each of the four conditions, using the D16 membrane diffractometer instruments at the Institut Laue-Langevin, Grenoble, France. The scanning protocol consisted of θ–2θ scans at $\pm 2°$ around the predicted Bragg angle of the first five orders of diffraction.

Data analysis

The diffraction intensity was obtained from the detector counts according to the pixel response, and the diffraction images were then collapsed into a linear spectrum for each scan using D16 instrument software *Lamp* (47). Baseline correction and peak fitting based on the Lorentz function were performed using *PeakFit* (AISN Software). The diffraction angles and intensities determined by the peak fitting were then transferred into *Excel* (Microsoft) spreadsheets for geometric correction. The data collected at 8%

^2H_2O were combined to construct a continuous transform function, from which sets of structure factors were extracted to be used in the calculation of neutron- scattering density maps. Each map, representing a one-dimensional bilayer profile, was constructed using Fourier summation in which the diffraction data of each order contribute a frequency cosine function. The square roots of the intensities were taken to produce the structure factor amplitudes. Because the net neutron scattering length density of water containing 8% deuterium is zero, a single continuous transform function fits all structure factors collected with water of this composition, no matter what the *d*-repeat spacing. All structure factors collected at 8% ^2H_2O data were plotted, and the phase angles for each diffraction order were adjusted to allow the observed points of the three data sets to fit a single continuous transformation, using a least-squares minimization procedure (45). Water profiles of the stacked bilayer systems were calculated by subtracting the scattering profile at 8% ^2H_2O from the profile at 50% ^2H_2O. Scaling of the individual data sets to each other was performed using an absolute scale based on the neutron- scattering lengths of known component molecules, i.e., phospholipids.

RESULTS

Circular dichroism spectroscopy

To investigate the folding of the N-terminal domain of annexin A1 in the absence and presence of vesicles, the secondary structure of rat annexin A1(2–26) peptide was assessed using CD spectroscopy with/without unilamellar DMPC/DMPS vesicles (3:1 molar ratio) at 20°C (Fig. 2). In aqueous buffer, the CD spectrum of rat annexin A1(2–26) displayed a typical spectrum characteristic for predominantly random-coil conformation. However, in the presence of SUVs, the CD spectrum revealed a maximum at 190 nm and two minima at 208 and 222 nm, which is a typical spectrum for α-helical conformation. Secondary structure prediction indicates a 58% increase in α-helix structure. These results demonstrate that the association of the peptide with phospholipid vesicles induces formation of helical structure in the peptide.

Lateral surface pressure measurement

We used a surface film balance with Langmuir Blodgett phospholipid monolayers to monitor the binding kinetics of annexin proteins and A1 N-terminal peptides in the absence of calcium. Basically, both transmembrane domains (48) and amphipathic helices (49) of proteins would cause an increase in surface pressure of phospholipid monolayer because a substantial area of phospholipids on the water surface is occupied by the inserted side chains. The surface pressure of DMPC/DMPS monolayers (3:1 molar ratio) after injection of full-length proteins or peptides was recorded as a function of time. As seen in Fig. 3 *a*, full-length human annexin A1 induced a dramatic surface pressure increase of 3 mN/m in the initial 200 s. This result agrees with a previous study, which also demonstrated that the calcium-independent interaction of annexin A1 is based on hydrophobic interactions and independent of the charge of the phospholipid headgroups (20). As expected, human annexin A5 lacking the membrane-binding function in its N-terminal domain showed no monolayer penetration ability. Chimera annexin $A1_N$-$A5_C$ also gave rise to an increase in surface pressure, although to a lesser extent than annexin A1 (~2 mN/m). The increase in surface pressure seen with the chimera, but not with annexin A5, provides further proof that the N-terminal

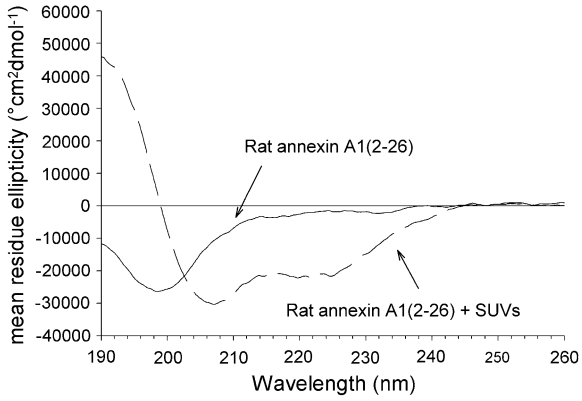

FIGURE 2 CD spectra of rat annexin A1(2–26) in the absence (*solid line*) and presence (*dashed line*) of DMPC/DMPS (3:1 molar ratio) SUVs.

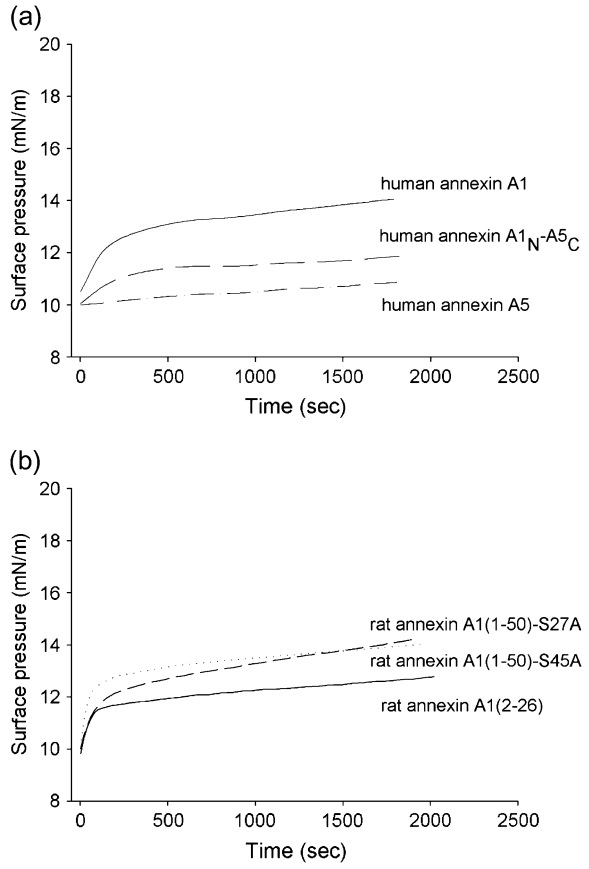

FIGURE 3 Phospholipid monolayer surface pressure measurements after injection of (*a*) full-length human annexin proteins: annexin A1 (*solid line*), annexin A5 (*dash-dotted line*), and chimera protein annexin $A1_N$-$A5_C$ (*dashed line*), and (*b*) rat annexin A1 N-terminal peptides (1–50)-S27A (*dashed line*), (1–50)-S45A (*dotted line*), and (2–26) (*solid line*) in the absence of calcium. Baseline traces acquired in the absence of peptides or proteins have been subtracted.

domain of annexin A1 exerts independent membrane interactions, although annexin A5 seems to have a low monolayer penetration ability, most likely because of nonspecific electrostatic interactions. The difference in the surface pressure curves of annexin A1 and the chimera indicates that the C-terminal domain affects the overall membrane association of the full-length proteins, probably by structurally stabilizing the conformation of the N-terminal domain in a way that would enable productive membrane interactions. However, eventual calcium-independent interactions of the C-terminal domain of annexin A1 with the monolayer cannot be excluded by our current results.

To validate the function of isolated N-terminal domains in monolayer association, several rat annexin A1 peptides also were subjected to surface pressure measurements in the absence of calcium (Fig. 3 *b*). The rat peptides (1–50)-S27A and (1–50)-S45A revealed similar levels of surface pressure increase when compared with full-length annexin A1 and the chimera for the entire time course of ~2000 s (~3 mN/m). The slightly slower time course of adsorption to the monolayer in the case of (1–50)-S27A might be explained by the stabilizing effect of Ser-27 on the preceding helical structure. Situated at the cap of the α-helix, the side-chain hydroxyl group of Ser-27 is likely to interact with a backbone carbonyl group of the α-helix, similar to the situation observed in porcine full-length annexin A1 (1hm6) where Ser-28-OH is hydrogen-bonded to the carbonyl group of Val-25. Such an interaction would be lacking in (1–50)-S27A and thus yield a less stable α-helical structure because of the higher flexibility of the cap, which could explain the slower adsorption process.

A surface pressure increase of rat annexin A1(2–26) was also observed, but with ~2 mN/m less intensity than with the other two mutant peptides. The difference in surface pressure increase of this peptide as compared with the longer peptides (residues 1–50) is most likely caused by additional interactions with the monolayer by residues 27–50.

Neutron diffraction

The lamellar spacings (*d*-repeats) of the DMPC/DMPS (3:1 molar ratio) bilayer at 90% relative humidity were determined by least- squares fitting to the five orders of neutron diffraction. As shown in Table 1, the *d*-repeats do not change significantly after addition of 1 mol % annexin A1 N-terminal peptides. Furthermore, human and rat peptides reveal no significant differences in lamellar spacings. The fact that the unit cell dimension in the *Z*-direction does not change on addition of the peptides rules out the possibility of superficial interaction of peptide and lipid. These results suggest an insertion of the annexin A1 N-terminal peptides into the phospholipid monolayer or accommodation of the peptides in the hydrophilic spaces between the stacked bilayers: either the peptides lie parallel to the bilayer surface (Fig. 4), or they insert vertically into the bilayer.

TABLE 1 Lamellar spacings (*d*-repeats) of the DMPC/DMPS (3:1 molar ratio) bilayer in the presence or absence of annexin A1 N-terminal peptides

	d-Repeat (Å)
DMPC/DMPS	54.45
DMPC/DMPS + 1 mol % human annexin A1(1–21)	54.52
DMPC/DMPS + 1 mol % rat annexin A1(2–26)	54.45

Neutron structure factors for each order of diffraction have been calculated and are shown in Table 2. From these, neutron-scattering density profiles of the DMPC/DMPS bilayer, in the presence or absence of the peptides, were calculated (Fig. 5). At 8% ^2H_2O composition, the mean neutron scattering length of the water mixture is zero (50), so the water does not contribute to the profiles shown. The trace shown with a solid line represents the section of the neutron scattering length density profile of the phospholipid bilayer along the *Z*-axis, perpendicular to the surface of the lipid bilayer. The two maxima of the profile arise from a combination of the phosphate-containing head groups and the hydrogen-poor glycerol groups, whereas the minimum in the center indicates the hydrogen-rich methyl groups at the bilayer center. The short-dashed trace, obtained by subtracting structure factors for lipid bilayer- containing peptide from structure factors for pure lipid, followed by Fourier transformation, describes the difference profile of human annexin A1(1–21) (Fig. 5 *a*) and rat annexin A1(2–26) (Fig. 5 *b*).

To obtain more quantitative measurements of the changes induced by the annexin A1 N-terminal peptides in the bilayer structure, the difference profiles were fitted to a single pair of Gaussians. The fitting was carried out in reciprocal space to avoid artifacts caused by series termination error. The fit parameters are summarized in Table 3. It is noteworthy that, in each case, the difference was adequately described by a

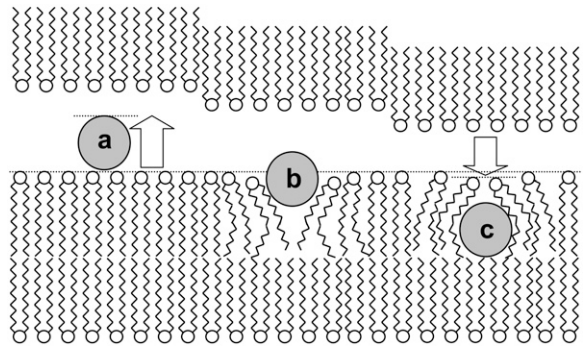

FIGURE 4 Incorporation of a helical peptide into a stacked bilayer system can affect the *d*-repeat distance by altering the height of the bilayer water layer. If the peptide lies along the bilayer surface (*a*), the water layer becomes thicker because it now has to include the peptide and its hydration shell. When the peptide lies deep in the bilayer (*c*), rearrangement of the phospholipid molecules to incorporate the peptide can increase their horizontal width, thereby decreasing their vertical height. If the *d*-repeat does not change, this indicates that the peptide lies in the interfacial region (*b*), such that any water layer thickening is compensated for by bilayer thinning.

TABLE 2 Neutron structure factors $F(h)$ of the annexin A1 N-terminal peptides in the bilayer DMPC/DMPS (3:1 molar ratio)

	$F(1)$	$F(2)$	$F(3)$	$F(4)$	$F(5)$
DMPC/DMPS	–20.59	–5.76	8.68	–6.04	–2.14
DMPC/DMPS + human annexin A1(1–21)	–22.83	–6.31	10.56	–5.89	–1.98
DMPC/DMPS + rat annexin A1(2–26)	–22.96	–6.38	10.17	–6.91	–2.50

h stands for the diffraction order. Data were collected at 90% relative humidity, 8% ^2H_2O, 26°C.

TABLE 3 Parameters of the Gaussian fits of the peptide difference profiles in reciprocal space

	Scattering length (10^{-13} cm)	Position (Å)	Width (Å)
Human annexin A1(1–21)	1.24	19.05	9.42
Rat annexin A1(2–26)	1.29	19.36	8.56

The position is expressed as the distance from the center of the bilayer. Width is the full width at half height of the fitted Gaussian distribution.

single pair of Gaussians, indicating that the minor peaks located at the bilayer center are artifacts, produced by termination error. Each of the peptides appears at the interface of the phospholipid head groups and alkyl chains, the narrow width suggesting a parallel orientation relative to the bilayer surface. The Gaussian peaks characterizing the human and rat peptides are positioned at 19.05 Å and 19.36 Å, respectively, very close to the maxima representing the head groups and glycerol groups of the phospholipids.

The water distribution in the stacked bilayer system was obtained by subtracting the scattering profile at 8% ^2H_2O from that at 25% ^2H_2O sample hydration. Fig. 6 shows the water distribution profiles in the pure lipid bilayer as well as in the presence of the human and rat peptides. The split peaks at the ends of the figure (can be seen as a single peak for continuous extension of unit cells) represent the water between two adjacent lipid bilayers. The three difference profiles are very similar to each other, apart from minor features in the lipid core region in the two peptide-containing samples. To validate the profiles, Gaussian peaks were fitted in reciprocal space. The results, shown in Table 4, clearly indicate that the features at ~11 Å are real, although a minor component exists, accounting for only 1–1.5% of the total water. The peak located at the bilayer center (at $Z = 0$) does not fit to a Gaussian (in reciprocal-space fitting), indicating that it results from termination error. The minor peaks are readily explained in terms of exchanged protons on the hydrophobic surface of the amphipathic α-helix bound parallel to the bilayer surface and the deuterium atoms on the hydrophobic face caused by hydrogen/deuterium exchange from solvent leading to higher scattering length (51,52). Most importantly, the minor peaks shown here cannot be explained by a transmembrane model in which the peptide forms a channel-like structure lying perpendicular to the bilayer and ^2H_2O diffusing freely through the bilayer (53). The perpendicular insertion model should appear as a continuous bulge across the bilayer.

With the data from Tables 3 and 4 and the bilayer center taken as the origin, a straightforward calculation shows that the

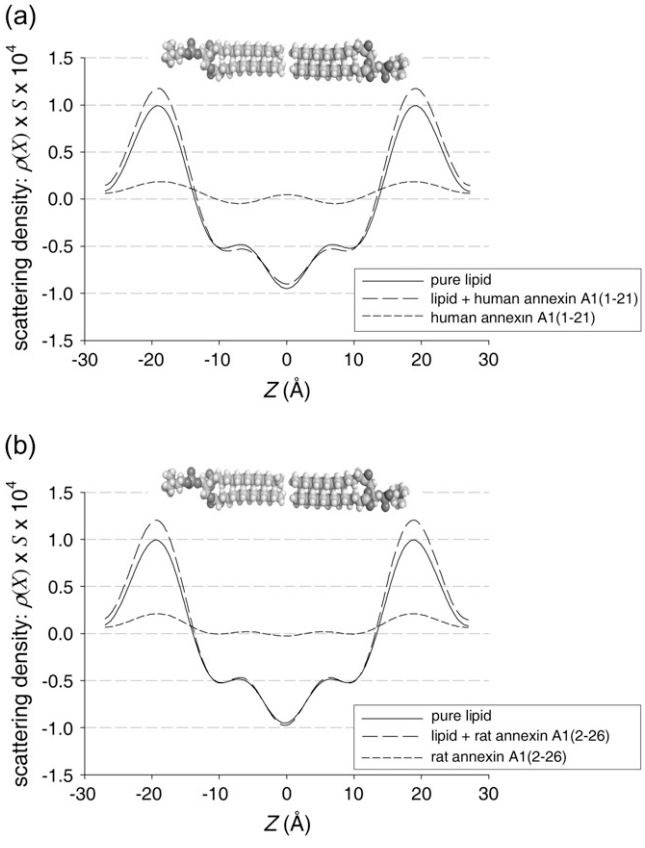

FIGURE 5 Neutron- scattering profiles of DMPC/DMPS (3:1 molar ratio) in the presence of 1% (*a*) human annexin A1(1–21) and (*b*) rat annexin A1(2–26) peptides. Experiments were carried out in 8% ^2H_2O, at 92% relative humidity. A pair of lipid molecules at the bottom is shown for orientation.

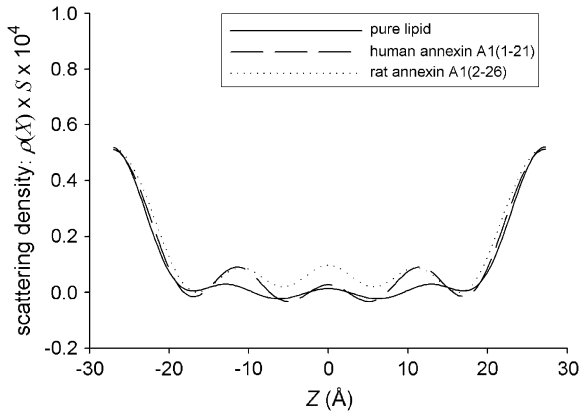

FIGURE 6 Water distribution profiles of DMPC/DMPS (3:1 molar ratio) in the absence (*solid line*) and presence of human annexin A1(1–21) (*dashed line*) and rat annexin A1(2–26) (*dotted line*).

TABLE 4 Parameters of the Gaussian fits of the water distribution in reciprocal space

	Scattering length (10^{-13} cm)	Position (Å)	Width (Å)
Pure lipid	2.35	25.17	7.06
Human annexin A1(1–21)			
1st Gaussian	2.75	25.05	7.18
2nd Gaussian	0.37	11.64	5.46
Rat annexin A1(2–26)			
1st Gaussian	2.46	24.76	8.26
2nd Gaussian	0.25	10.66	5.32

The position is expressed as the distance from the center of the bilayer. Width is the full width at half height of the fitted Gaussian distribution.

peptide peaks (full width at half height) span from 14.34 to 23.76 Å (human peptide) and 15.08 to 23.64 Å (rat peptide). Similarly, the inner edges of water at half height lie at 21.46 Å (human peptide) and 20.63 Å (rat peptide). This means that each of the peptides lies in a region of steep hydrophobic gradient, ranging from the alkyl chains to the solvated head groups, similar to other amphipathic α-helical peptides (54,55). Although the outer edge of each peptide is positioned at a similar depth in the bilayer (23.76 Å and 23.64 Å for human and rat peptide, respectively), it should be noted that the full width of human annexin A1(1–21) (9.42 Å) is larger than that of rat annexin A1(2–26) (8.56 Å). The x-ray structure of porcine annexin A1 in the absence of calcium (32) shows that the N-terminal helical domain has a kink at Glu-17. Human annexin A1(1–21) has an identical amino acid sequence compared with the porcine ortholog, except for residue 17 being an aspartate. If it is assumed that the human peptide adopts a similar conformation to the porcine protein, then this would explain its greater width in neutron scattering profiles.

DISCUSSION

Previous studies showed that the N-terminal domain of some annexins can adopt an α-helical conformation, and the helices seem to have amphipathic character. The crystal structure of human annexin A1(2–15) in complex with the E-F hand protein S100A11 revealed an amphipathic helix for the peptide in which the hydrophobic residues are buried within the complex and in contact with the C-terminal helix of S100A11 (56). In contrast, the hydrophilic residues are involved in the hydrogen bond with the N-terminal helix of S100A11.

NMR and CD studies demonstrated that Val-4 to Glu-19 of human annexin A1(2–26) peptide adopt a mainly α-helical conformation in membrane-mimic systems (34). Intriguingly, the induction of α-helical secondary structure on addition of TFE has also been observed with human annexin A2(1–31) (57). However, detailed molecular information about the interaction of the annexin N-terminal domains with membranes remains unclear so far.

Results from our CD experiments show that α-helical secondary structure is induced in annexin A1 N-terminal peptide (residues 2–26) in the presence of phospholipid membrane, which agrees very well with previously published studies. Together, these results suggest that the N-terminal domain of annexin A1 retains the structure of an amphipathic α-helix when expelled from the C-terminal domain and interacting with a membrane.

The monolayer lateral surface pressure measurements of full-length annexins A1 and A5 are in excellent agreement with previous studies (20) and, together with the data for the $A1_N$-$A5_C$ chimera, confirm that the calcium-independent membrane interaction of annexin A1 is caused by the properties of its N-terminal domain. The N-terminal domains of rat and human annexin A1 share 80% similarity and have been shown to be able to cause liposome aggregation (27). The two mutant peptides S27A and S45A were originally synthesized to block the phosphorylation sites on the N-terminal domain. The results shown here demonstrate that all three peptides are able to interact with the membrane directly, independent of calcium ions. Although annexins generally require acidic phospholipids for their canonical membrane binding, the secondary membrane binding site of annexin A1 shows no such preference (24,25). The pI values for rat annexin A1(2–26), (1–50)-S27A, and (1–50)-S45A are 4.7, 4.8, and 4.8, respectively. Under the experimental conditions of pH 6, the peptides thus possess negative charge but still associate with the PS-containing phospholipid mixture. It can therefore be concluded that the interactions are hydrophobic rather than electrostatic, which agrees with the parallel arrangement of an amphipathic helix to the membrane bilayer surface.

Structural details of the membrane-bound state of annexin A1 N-terminal peptides were obtained in this study by neutron diffraction using multiple membrane bilayer stacks. The results unambiguously showed that the peptides adopt a peripheral mode of binding and are oriented parallel to the membrane surface. The diffraction experiments were analyzed as to the difference scattering density profiles as well as the water distribution in the stacked bilayer system. The scattering density profiles obtained for the peptides, as well as the water distribution, showed no sign of any additional component appearing in the inner regions of the bilayer.

An increase in surface pressure of lipid monolayers is generally interpreted as a penetration of the membrane surface (59). Calculation of the axial location of the membrane-bound peptides from the scattering profiles reveals that the peptides extend from the alkyl chains to the solvated head groups of the phospholipid molecules. Accordingly, the membrane-adjacent side chains of the annealed α-helix insert into the membrane surface region, thus providing an explanation for the increase in surface pressure.

Clarification of the membrane aggregation mechanism of annexin A1 will depend on the structural information about the membrane-bound state of the full-length protein. However, in the absence of such data, it seems reasonable, based on the current knowledge, to assume that the isolated N-terminal peptides show a similar behavior as when covalently attached

to the C-terminal domain. Based on this assumption, the current results put further weight on the notion that the annexin A1 membrane aggregation mechanism, under the environmental parameters of this study, involves two simultaneous binding sites on one annexin molecule: the canonical calcium-dependent binding via the convex surface and the calcium-independent binding via the membrane-intercalated α-helical N-terminal domain. A further interesting problem in this context is the conformational state of the N-terminal domain of annexin A1 during the relocation process from the protein-harbored conformation to the membrane-associated state.

The previously published concept of amphitropism describes the phenomenon of a protein localizing to an aqueous compartment in one form and reversibly attaching to a membrane in another form (60). In this concept, annexin A1 fits well within one class together with proteins such as cytidyltransferase, factor VIII, vinculin, and others (61). All these proteins share the common feature of responding to an increase in negative charge density at the membrane, and for some of them, sensitivity to membrane curvature and packing pressure has been implicated. Intriguingly, an implication of annexins in membrane curvature has been reported earlier (62), and recent studies about annexin B12 (63) seem to bring this link back into focus. However, contributions by different membrane binding sites, as are likely to be the case for annexin A1, need to be clearly distinguished.

Our current results support the fundamental importance of the annexin A1 N-terminal domain for membrane association as shown by immunofluorescence (64), although the effect of phosphorylation on the molecular mechanism of the annexin A1 N-terminal domain remains to be elucidated in more detail. Further studies elucidating the structure of membrane-bound full-length annexin A1 will be required to validate and extend the current hypothesis and are currently under way in our laboratories.

CONCLUSION

Results from the current study support the hypothesis that annexin A1 might interact with two adjacent membranes simultaneously. Using N-terminal peptides of annexin A1, we have been able to show that an α-helical secondary structure is induced by the binding of the peptides to phospholipid membranes. Structural information from neutron scattering enabled us to determine the location of the peptides in the membrane-bound state. The peptides form an amphipathic helix where some side chains intercalate with the phospholipids, and the helix axis lies parallel to the membrane surface.

A.H. gratefully acknowledges partial support of this study by the Royal Society (London) and the European League Against Rheumatism (EULAR).

REFERENCES

1. Gerke, V., C. E. Creutz, and S. E. Moss. 2005. Annexins: linking Ca^{2+} signalling to membrane dynamics. *Nat. Rev. Mol. Cell Biol.* 6:449–461.
2. Gerke, V., and S. E. Moss. 2002. Annexins: from structure to function. *Physiol. Rev.* 82:331–371.
3. Klee, C. B. 1988. Ca^{2+}-dependent phospholipid- (and membrane-) binding proteins. *Biochemistry.* 27:6645–6653.
4. Burgoyne, R. D., and M. J. Geisow. 1989. The annexin family of calcium-binding proteins. *Cell Calcium.* 10:1–10.
5. Swairjo, M. A., and B. A. Seaton. 1994. Annexin structure and membrane interactions: a molecular perspective. *Annu. Rev. Biophys. Bioeng.* 23:193–213.
6. Hofmann, A., and R. Huber. 2003. Structural conservation and functional versatility: Allostery as a common annexin feature. In Annexins: Biological importance and annexin-related pathologies. J. Bandorowicz-Pikula, editor. Landes Bioscience, Georgetown, TX. 38–60.
7. Hayes, M. J., D. Shao, M. Bailly, and S. E. Moss. 2006. Regulation of actin dynamics by annexin 2. *EMBO J.* 25:1816–1826.
8. Babiychuk, E. B., and A. Draeger. 2000. Annexins in cell membrane dynamics: Ca^{2+}-regulated association of lipid microdomains. *J. Cell Biol.* 150:1113–1124.
9. Babiychuk, E. B., and A. Draeger. 2006. Regulation of ecto-5′-nucleotidase activity via Ca^{2+}-dependent, annexin 2-mediated membrane rearrangement? *Biochem. Soc. Trans.* 34:374–376.
10. Geisow, M. J., U. Fritsche, J. M. Hexham, B. Dash, and T. Johnson. 1986. A consensus amino-acid sequence repeat in *Torpedo* and mammalian Ca^{2+}-dependent membrane-binding proteins. *Nature.* 320:636–638.
11. Huber, R., M. Schneider, I. Mayr, J. Romisch, and E. P. Paques. 1990. The calcium binding sites in human annexin V by crystal structure analysis at 2.0 A resolution. Implications for membrane binding and calcium channel activity. *FEBS Lett.* 275:15–21.
12. Huber, R., R. Berendes, A. Burger, M. Schneider, A. Karshikov, H. Luecke, J. Romisch, and E. Paques. 1992. Crystal and molecular structure of human annexin V after refinement. Implications for structure, membrane binding and ion channel formation of the annexin family of proteins. *J. Mol. Biol.* 223:683–704.
13. Swairjo, M. A., N. O. Conch, M. A. Kaetzel, J. R. Dedman, and B. A. Seaton. 1995. Ca^{2+}-bridging mechanism and phospholipid head group recognition in the membrane-binding protein annexin V. *Nat. Struct. Biol.* 2:968–974.
14. Montaville, P., J. M. Neumann, F. Russo-Marie, F. Ochsenbein, and A. Sanson. 2002. A new consensus sequence for phosphatidylserine recognition by annexins. *J. Biol. Chem.* 277:24684–24693.
15. Naka, M., Z. X. Qing, T. Sasaki, H. Kise, I. Tawara, S. Hamaguchi, and T. Tanaka. 1994. Purification and characterization of a novel calcium-binding protein, S100C, from porcine heart. *Biochim. Biophys. Acta.* 1223:348–353.
16. Seemann, J., K. Weber, and V. Gerke. 1996. Structural requirements for annexin I-S100C complex-formation. *Biochem. J.* 319:123–129.
17. Zobiack, N., V. Gerke, and U. Rescher. 2001. Complex formation and submembranous localization of annexin 2 and S100A10 in live HepG2 cells. *FEBS Lett.* 500:137–140.
18. Sudo, T., and H. Hidaka. 1998. Regulation of calcyclin (S100A6) binding by alternative splicing in the N-terminal regulatory domain of annexin XI isoforms. *J. Biol. Chem.* 273:6351–6357.
19. Parente, L., and E. Solito. 2004. Annexin 1: more than an anti-phospholipase protein. *Inflamm. Res.* 53:125–132.
20. Rosengarth, A., A. Wintergalen, H. Galla, H. Hinz, and V. Gerke. 1998. Ca^{2+}-independent interaction of annexin I with phospholipid monolayers. *FEBS Lett.* 438:279–284.
21. Meers, P., T. Mealy, N. Pavlotsky, and A. I. Tauber. 1992. Annexin I-mediated vesicular aggregation: mechanism and role in human neutrophils. *Biochemistry.* 31:6372–6382.
22. Meers, P., T. Mealy, and A. I. Tauber. 1993. Annexin I interactions with human neutrophil specific granules: fusogenicity and coaggregation with plasma membrane vesicles. *Biochim. Biophys. Acta.* 1147:177–184.
23. Lee, G., and H. B. Pollard. 1997. Highly sensitive and stable phosphatidylserine liposome aggregation assay for annexins. *Anal. Biochem.* 252:160–164.

24. Andree, H. A., G. M. Willems, R. Hauptmann, I. Maurer-Fogy, M. C. Stuart, W. T. Hermens, P. M. Frederik, and C. P. Reutelingsperger. 1993. Aggregation of phospholipid vesicles by a chimeric protein with the N-terminus of annexin I and the core of annexin V. *Biochemistry*. 32:4634–4640.
25. Bitto, E., M. Li, A. M. Tikhonov, M. L. Schlossman, and W. Cho. 2000. Mechanism of annexin I-mediated membrane aggregation. *Biochemistry*. 39:13469–13477.
26. Kastl, K., A. Herrig, E. Luthgens, A. Janshoff, and C. Steinem. 2004. Scrutiny of annexin A1 mediated membrane-membrane interaction by means of a thickness shear mode resonator and computer simulations. *Langmuir*. 20:7246–7253.
27. Seemann, J., K. Weber, M. Osborn, R. G. Parton, and V. Gerke. 1996. The association of annexin I with early endosomes is regulated by Ca^{2+} and requires an intact N-terminal domain. *Mol. Biol. Cell*. 7:1359–1374.
28. Bitto, E., and W. Cho. 1999. Structural determinant of the vesicle aggregation activity of annexin I. *Biochemistry*. 38:14094–14100.
29. Creutz, C. E., and D. C. Sterner. 1983. Calcium dependence of the binding of synexin to isolated chromaffin granules. *Biochem. Biophys. Res. Commun*. 114:355–364.
30. de la Fuente, M., and A. V. Parra. 1995. Vesicle aggregation by annexin I: role of a secondary membrane binding site. *Biochemistry*. 34:10393–10399.
31. Lambert, O., V. Gerke, M. F. Bader, F. Porte, and A. Brisson. 1997. Structural analysis of junctions formed between lipid membranes and several annexins by cryo-electron microscopy. *J. Mol. Biol*. 272:42–55.
32. Rosengarth, A., V. Gerke, and H. Luecke. 2001. X-ray structure of full-length annexin 1 and implications for membrane aggregation. *J. Mol. Biol*. 306:489–498.
33. Rosengarth, A., and H. Luecke. 2003. A calcium-driven conformational switch of the N-terminal and core domains of annexin A1. *J. Mol. Biol*. 326:1317–1325.
34. Yoon, M. K., S. H. Park, H. S. Won, D. S. Na, and B. J. Lee. 2000. Solution structure and membrane-binding property of the N-terminal tail domain of human annexin I. *FEBS Lett*. 484:241–245.
35. Alvarez-Martinez, M. T., J. C. Mani, F. Porte, C. Faivre-Sarrailh, J. P. Liautard, and J. Sri Widada. 1996. Characterisation of the interaction between annexin I and profilin. *Eur. J. Biochem*. 238:777–784.
36. Lim, L. H. K., E. Solito, F. Russo-Marie, R. J. Flower, and M. Perretti. 1998. Promoting detachment of neutrophils adherent to murine postcapillary venules to control inflammation—effect of lipocortin 1. *Proc. Natl. Acad. Sci. USA*. 95:14535–14539.
37. Burger, A., R. Berendes, D. Voges, R. Huber, and P. Demange. 1993. A rapid and efficient purification method for recombinant annexin V for biophysical studies. *FEBS Lett*. 329:25–28.
38. Hofmann, A., J. Proust, A. Dorowski, R. Schantz, and R. Huber. 2000. Annexin 24 from *Capsicum annuum*. X-ray structure and biochemical characterization. *J. Biol. Chem*. 275:8072–8082.
39. Dabitz, N., N. J. Hu, A. M. Yusof, N. Tranter, A. Winter, M. Daley, O. Zschörnig, A. Brisson, and A. Hofmann. 2005. Structural determinants for plant annexin-membrane interactions. *Biochemistry*. 44:16292–16300.
40. Szoka, F. J., and D. Papahadjopoulos. 1980. Comparative properties and methods of preparation of lipid vesicles (liposomes). *Annu. Rev. Biophys. Bioeng*. 9:467–508.
41. Pagano, R. E., and J. N. Weinstein. 1978. Interactions of liposomes with mammalian cells. *Annu. Rev. Biophys. Bioeng*. 7:435–468.
42. Hofmann, A., and A. Wlodawer. 2002. PCSB–a program collection for structural biology and biophysical chemistry. *Bioinformatics*. 18:209–210.
43. Hu, N.-J., M. Currid, M. Daley, and A. Hofmann. 2005. Automated CD and fluorescence data processing with ACDP and AFDP. *Appl. Spectrosc*. 59:68A.
44. Mukhopadhyay, S., and W. Cho. 1996. Interactions of annexin V with phospholipid monolayers. *Biochim. Biophys. Acta*. 1279:58–62.
45. Darkes, M. J., and J. P. Bradshaw. 2000. Real-time swelling-series method improves the accuracy of lamellar neutron-diffraction data. *Acta Crystallogr. D Biol. Crystallogr*. D56:48–54.
46. Balali-Mood, K., R. H. Ashley, T. Hauss, and J. P. Bradshaw. 2005. Neutron diffraction reveals sequence-specific membrane insertion of pre-fibrillar islet amyloid polypeptide and inhibition by rifampicin. *FEBS Lett*. 579:1143–1148.
47. Richard, D., M. Ferrand, and G. J. Kearley. 1996. LAMP, Large Array Manipulation Program (2001 version). http://www.ill.fr/data_treat/lamp/front.html.
48. Zheng, S., J. Strzalka, C. Ma, S. J. Opella, B. M. Ocko, and J. K. Blasie. 2001. Structural studies of the HIV-1 accessory protein Vpu in Langmuir monolayers: synchrotron x-ray reflectivity. *Biophys. J*. 80:1837–1850.
49. Datta, G., M. Chaddha, S. Hama, M. Navab, A. M. Fogelman, D. W. Garber, V. K. Mishra, R. M. Epand, R. F. Epand, S. Lund-Katz, M. C. Phillips, J. P. Segrest, and G. M. Anantharamaiah. 2001. Effects of increasing hydrophobicity on the physical-chemical and biological properties of a class A amphipathic helical peptide. *J. Lipid Res*. 42:1096–1104.
50. King, G. I., and S. H. White. 1986. Determining bilayer hydrocarbon thickness from neutron diffraction measurements using strip-function models. *Biophys. J*. 49:1047–1054.
51. Hvidt, A., and S. O. Nielsen. 1966. Hydrogen exchange in proteins. *Adv. Protein Chem*. 21:287–386.
52. Hvidt, A., and K. Linderstrom-Lang. 1954. Exchange of hydrogen atoms in insulin with deuterium atoms in aqueous solutions. *Biochim. Biophys. Acta*. 14:574–575.
53. Bradshaw, J. P. 1997. Phosphatydylglycerol promotes bilayer insertion of salmon calcitonin. *Biophys. J*. 72:2180–2186.
54. Davies, S. M., T. A. Harroun, T. Hauss, S. M. Kelly, and J. P. Bradshaw. 2003. The membrane bound N-terminal domain of human adenosine diphosphate ribosylation factor-1 (ARF1). *FEBS Lett*. 548:119–124.
55. Bradshaw, J. P., K. C. Duff, P. J. Gilchrist, and A. M. Saxena. 1996. Neutron diffraction studies of amphipathic helices in phospholipid bilayers. *Basic Life Sci*. 64:191–202.
56. Rety, S., D. Osterloh, J. P. Arie, S. Tabaries, J. Seeman, F. Russo-Marie, V. Gerke, and A. Lewit-Bentley. 2000. Structural basis of the $Ca2^{+}$-dependent association between S100C (S100A11) and its target, the N-terminal part of annexin I. *Structure*. 8:175–184.
57. Hong, Y. H., H. S. Won, H. C. Ahn, and B. J. Lee. 2003. Structural elucidation of the protein- and membrane-binding properties of the N-terminal tail domain of human annexin II. *J. Biochem*. 134:427–432.
58. Reference deleted in proof.
59. Newman, R., A. Tucker, C. Ferguson, D. Tsernoglou, K. Leonard, and M. J. Crumpton. 1989. Crystallization of p68 on lipid monolayers and as three-dimensional single crystals. *J. Mol. Biol*. 206:213–219.
60. Burn, P. 1988. Amphitropic proteins: a new class of membrane proteins. *Trends Biochem. Sci*. 13:79–83.
61. Johnson, J. E., and R. B. Cornell. 1999. Amphitropic proteins: regulation by reversible membrane interactions. *Mol. Membr. Biol*. 16:217–235.
62. Kinnunen, P. K. J. 1996. On the molecular level mechanisms of peripheral protein-membrane interactions induced by lipids forming inverted non-lamellar phases. *Chem. Phys. Lipids*. 81:151–166.
63. Fischer, T., L. Lu, H. T. Haigler, and R. Langen. 2007. Annexin B12 is a sensor of membrane curvature and undergoes major curvature-dependent structural changes. *J. Biol. Chem*. 282:9996–10004.
64. Solito, E., H. C. Christian, M. Festa, A. Mulla, T. Tierney, R. J. Flower, and J. C. Buckingham. 2006. Post-translational modification plays an essential role in the translocation of annexin A1 from the cytoplasm to the cell surface. *FASEB J*. 20:1498–1500.
65. Hennig, L. 1999. WinGene/WinPep: user-friendly software for the analysis of amino acid sequences. *Biotechniques*. 26:1170–1172.